Elastic Cross Sections for Low-Energy e^-–CH_4 Collisions

L. E. Machado[1], M.-T. Lee[2] and L. M. Brescansin[3]

[1] *Departamento de Física, UFSCar, 13565-905, São Carlos, SP, Brazil*

[2] *Departamento de Química, UFSCar, 13565-905, São Carlos, SP, Brazil*

[3] *Instituto de Física "Gleb Wataghin", UNICAMP, 13083-970, Campinas, SP, Brazil*

Received February 12, 1998

Recently we have extended our codes based on the Schwinger variational iterative method in order to study elastic electron scattering by non-planar molecules with symmetries reducible to the C_{2v} point group and also to include a correlation-polarization contribution to the electron-molecule interaction potential. In this work we report the first application of these newly extended codes to the calculation of cross sections for low-energy elastic scattering of electrons by methane. Differential, integral and momentum-transfer cross sections were calculated in the 0.1–50 eV incident energy range. Comparison of our results with the extensive available data, both experimental and theoretical, reveals the reliability of our method. Particularly, the Ramsauer minimum at around 0.4 eV and the resonance structure at around 8 eV are well reproduced in our calculations.

I. Introduction

Over the last fifteen years the Schwinger variational iterative method (SVIM) [1] has been widely used for calculations on elastic electron-molecule scattering [2-6] and molecular photoionization [1, 7-11]. Also, combined with the distorted-wave approximation, SVIM has been applied to the investigation of electronic excitation in molecules [12-18]. Besides its capability of treating electron scattering by both neutral and ionic molecular targets, SVIM has very solid theoretical grounds. It provides continuum wavefunctions that are shown to converge to the exact solutions of the specified projectile-target interaction potential being used [19]. Fully *ab-initio* calculations using SVIM have led to reliable cross sections and other related parameters over a large range of incident energies, from low (a few eV) to intermediate (up to a hundred eV) in a number of previous applications. However, except for a study on photoionization of methane [10] the use of SVIM has been limited to diatomic, linear and planar polyatomic molecular targets. In addition, those applications of the method have been restricted to the static-exchange (SE) level of approximation. On the other hand, accurate descriptions of the electron-molecule collision dynamics at the low and very-low (sub-eV) energy ranges usually require treatments beyond the SE level of approximation, namely, an appropriate balance of static, exchange and correlation-polarization potentials. We have recently extended our SVIM codes in order to treat nonplanar molecules with symmetry reducible to C_{2v}. Also, in this extended version a local correlation-polarization contribution to the electron-molecule interaction potential is included, following the prescription recommended by Padial and Norcross [20]. As a first application of the new version of our codes we studied the elastic e^-–CH_4 scattering in a wide incident energy range.

Methane is an interesting system on its own. It has been identified as a source of infrared absorption in the atmospheres of Jupiter and Saturn, and is a primary constituent of the atmospheres of outer planets such as Uranus and Neptune [21]. Also, methane is an important species in plasma processing [22] and plays a role in edge plasmas of fusion devices [23]. Secondly, electron collisions with methane are a very well studied problem, both experimentally and theoretically. Some pioneering experimental works reported in the 20's and

30's showed a deep minimum at around 0.4 eV and a broad maximum at 8 eV in the total cross sections [24-27]. These structures have also been seen in more recent measurements of elastic integral and momentum-transfer cross sections (ICS and MTCS) [28-34]. Differential cross sections (DCS) of elastically scattered electrons have also been extensively studied. Recent experimental data on DCS were reported in a number of works: Curry *et al.* [21], Tanaka *et al.* [28], Vuskovic and Trajmar [29], Sohn *et al.* [30], Shyn and Cravens [31], Boesten and Tanaka [32], Kanik *et al.* [33] and Mapstone and Newell [35], just to cite a few.

On the theoretical side, the literature is equally rich. DCS, MTCS as well as ICS for elastic e^-–CH_4 scattering have been calculated in the last fifteen years at different levels of approximation. Model potentials at static-exchange (SE) and at static-exchange-polarization (SEP) levels were used by several authors [36-39]. The Schwinger multichannel method using pseudopotentials was applied by Bettega *et al.* [40] to study elastic scattering of electrons by XH_4 molecules (X=C, Si, Ge, Pb). An exact SE calculation for elastic e^-–CH_4 scattering was reported by Lima *et al.* [41]. Beyond the exact-SE level, the correlation-polarization contributions to the interaction potential were taken into account either via an approximated local function [42,43] or via a multichannel treatment of the scattering equations [44,45].

In this work we use our newly extended version of the SVIM codes to calculate DCS, ICS and MTCS for elastic e^-–CH_4 scattering in the 0.1–50 eV energy range. The large amount of data provided by this calculation will be compared with the numerous results available in the literature. Our particular interest is to check if our method is capable, for instance, of describing correctly the structures in the ICS curve, namely, the Ramsauer minimum at very low energies and the broad resonance at around 8 eV. Once the reliability is firmly assured, our new codes will be applied to electron scattering by larger nonplanar systems.

The organization of the paper is as follows. In Sec. II we briefly discuss some aspects of the theory been used and in Sec. III we present some details of the computation. Our results are presented and compared with the available data in the literature in Sec. IV, where we also present short concluding remarks.

II. Theory and calculation

The Schrödinger equation for the continuum scattering orbitals can be written (in atomic units) as:

$$\left[-\nabla^2 + U(\vec{r}) - k^2 \right] \Psi_{\vec{k}}(\vec{r}) \;=\; 0 \qquad (1)$$

where $U(\vec{r}) \;=\; 2V(\vec{r})$ and $V(\vec{r})$ is the interaction potential between the target and the scattering electron. Eq. (1) can be converted into an equivalent Lippmann-Schwinger equation

$$\Psi^{(\pm)}_{\vec{k}} \;=\; \Phi_{\vec{k}} + G_0^{(\pm)} U \Psi^{(\pm)}_{\vec{k}} \qquad (2)$$

with $G_0^{(\pm)}$ being the free-particle Green's operator with outgoing- ($G_0^{(+)}$) or incoming-wave ($G_0^{(-)}$) boundary conditions. In order to take advantage of the symmetry of the target, the scattering wavefunctions can be partial-wave expanded as:

$$\Psi^{(\pm)}_{\vec{k}}(\vec{r}) \;=\; \left[\frac{2}{\pi}\right]^{\frac{1}{2}} \frac{1}{k} \sum_{p\mu lh} i^l \Psi^{(\pm)^{p\mu}}_{k,lh}(\vec{r}) X^{p\mu}_{lh}(\hat{k}). \qquad (3)$$

where $X^{p\mu}_{lh}(\hat{r})$ are generalized spherical harmonics, related to the usual spherical harmonics Y_{lm} by:

$$X^{p\mu}_{lh}(\hat{r}) \;=\; \sum_m b^{p\mu}_{lhm} Y_{lm}(\hat{r}). \qquad (4)$$

Here p is an irreducible representation (IR) of the molecular point group, μ is a component of this representation and h distinguishes between different bases of the same IR corresponding to the same value of l. The coefficients $b^{p\mu}_{lhm}$ satisfy important orthogonality conditions and are tabulated for the C_{2v} and O_h groups by Burke *et al.* [46]. The Schwinger variational expression for the T matrix can be written in the bilinear form as:

$$T^{(\pm)}_{\vec{k},\vec{k}_0} = < \Phi^{(\mp)}_{\vec{k}} \mid U \mid \tilde{\Psi}^{(\pm)}_{\vec{k}_0} > + < \tilde{\Psi}^{(\mp)}_{\vec{k}} \mid U \mid \Phi^{(\pm)}_{\vec{k}_0} > - < \tilde{\Psi}^{(\mp)}_{\vec{k}} \mid U - UG^{(\pm)}_0 U \mid \tilde{\Psi}^{(\pm)}_{\vec{k}_0} > \tag{5}$$

with $\tilde{\Psi}^{(\pm)}_{\vec{k}}$ denoting trial scattering wavefunctions . Using partial-wave expansions similar to (3) for both $\tilde{\Psi}^{(\pm)}_{\vec{k}}$ and the free-particle wave vector $\Phi^{(\pm)}_{\vec{k}}$, a partial wave on-shell T matrix (diagonal in both p and μ) is obtained:

$$T^{(\pm)^{p\mu}}_{k,lh;l'h'} = < \Phi^{(\mp)^{p\mu}}_{k,l'h'} \mid U \mid \tilde{\Psi}^{(\pm)^{p\mu}}_{k,lh} > + < \tilde{\Psi}^{(\mp)^{p\mu}}_{k,l'h'} \mid U \mid \Phi^{(\pm)^{p\mu}}_{k,lh} > - < \tilde{\Psi}^{(\mp)^{p\mu}}_{k,l'h'} \mid U - UG^{(\pm)}_0 U \mid \tilde{\Psi}^{(\pm)^{p\mu}}_{k,lh} > \tag{6}$$

where $k = \mid \vec{k}_0 \mid = \mid \vec{k} \mid$ for the elastic process.

The initial scattering wave functions can be expanded in a set R_0 of L^2 basis functions $\alpha_i(\vec{r}) = < \vec{r} \mid \alpha_i >$:

$$\tilde{\Psi}^{(\pm)^{p\mu}}_{k,lh}(\vec{r}) = \sum_{i=1}^{N} a^{(\pm)^{p\mu}}_{i,lh}(k)\alpha_i(\vec{r}) \tag{7}$$

Using (6) and (7), variational $T^{(\pm)^{p\mu}}_{k,lh;l'h'}$ matrix elements can be derived as:

$$T^{(\pm)^{p\mu}}_{k,lh;l'h'} = \sum_{i,j=1}^{N} < \Phi^{(\mp)^{p\mu}}_{k,l'h'} \mid U \mid \alpha_i > [D^{(\pm)^{-1}}]_{ij} < \alpha_j \mid U \mid \Phi^{(\pm)^{p\mu}}_{k,lh} > \tag{8}$$

where

$$D^{(\pm)}_{ij} = < \alpha_i \mid U - UG^{(\pm)}_0 U \mid \alpha_j > \tag{9}$$

and the corresponding approximate scattering solution with outgoing-wave boundary condition becomes:

$$\Psi^{(+)^{p\mu(S_0)}}_{k,lh}(\vec{r}) = \Phi^{p\mu}_{k,lh}(\vec{r}) + \sum_{i,j=1}^{M} < \vec{r} \mid G^{(+)}_0 U \mid \alpha_i > [D^{(+)^{-1}}]_{ij} < \alpha_j \mid U \mid \Phi^{p\mu}_{k,lh} > \tag{10}$$

Converged outgoing solutions of (2) can be obtained via an iterative procedure. The method consists in augmenting the basis set R_0 by the set

$$S_0 = \{\Psi^{(+)^{p\mu(S_0)}}_{k,l_1h_1}(\vec{r}), \Psi^{(+)^{p\mu(S_0)}}_{k,l_2h_2}(\vec{r}), ...\Psi^{(+)^{p\mu(S_0)}}_{k,l_ch_c}(\vec{r})\} \tag{11}$$

where l_c is the maximum value of l for which the expansion of the scattering solution (3) is truncated. A new set of partial wave scattering solutions can now be obtained from:

$$\Psi^{(+)^{p\mu(S_1)}}_{k,lh}(\vec{r}) = \Phi^{p\mu}_{k,lh}(\vec{r}) + \sum_{i,j=1}^{M} < \vec{r} \mid G^{(+)}U \mid \eta^{(S_0)}_i > [D^{(+)^{-1}}]_{ij} < \eta^{(S_0)}_j \mid U \mid \Phi^{p\mu}_{k,lh} > \tag{12}$$

where $\eta^{(S_0)}_i(\vec{r})$ is any function in the set $R_1 = R_0 \bigcup S_0$ and M is the number of functions in R_1. This iterative procedure continues until a converged $\Psi^{(+)^{p\mu(S_n)}}_{k,lh}(\vec{r})$ is achieved. These converged scattering wavefunctions correspond, in fact, to exact solutions of the truncated Lippmann-Schwinger equation with the potential U.

In an actual calculation we compute the converged partial wave K-matrix elements, $K^{p\mu(S_n)}_{k,lh;l'h'}$. These K-matrix elements can be obtained by replacing $D^{(+)}$ by its principal value, $D^{(P)}$, in Eq. (8). Hence, the corresponding partial-wave T-matrix elements can be calculated from

$$T^{p\mu(S_n)}_{k,lh,l'h'} = -\Big[\frac{2}{\pi}\Big] \sum_{l"h"} [1 - iK^{(S_n)}]^{p\mu}_{k,lh;l"h"} K^{p\mu(S_n)}_{k,l"h";l'h'} \tag{13}$$

By usual transformations, these matrix elements can be expressed in the laboratory frame (LF). The LF scattering amplitude $f(\hat{k}', \hat{k}'_0)$ is related to the T matrix by:

$$f(\hat{k}', \hat{k}'_0) \;=\; -2\pi^2 T, \tag{14}$$

where $\hat{k}'_0$ and $\hat{k}'$ are the directions of incident and scattered electron linear momenta, respectively. The differential cross section for elastic electron-molecule scattering is given by:

$$\frac{d\sigma}{d\Omega} \;=\; \frac{1}{8\pi^2}\int d\alpha sin\beta d\beta d\gamma |f(\hat{k}', \hat{k}'_0)|^2. \tag{15}$$

Here, (α, β, γ) are the Euler angles which define the orientation of the principal axes of the molecule. Finally, after some angular momentum algebra, the LF DCS averaged over the molecular orientations can be written as:

$$\frac{d\sigma}{d\Omega} \;=\; \sum_L A_L(k) P_L(cos\theta) \tag{16}$$

where θ is the scattering angle. The coefficients $A_L(k)$ in Eq. (16) are given by the formula

$$\begin{aligned} A_L(k) \;=\; & \frac{1}{2}\frac{1}{2L+1} \sum_{\substack{p\mu l h l' h' m m' \\ p_1 \mu_1 l_1 h_1 l'_1 h'_1 m_1 m'_1}} (-1)^{m'-m}\sqrt{(2l+1)(2l_1+1)}\times \\ & b^{p_1\mu_1}_{l'_1 h'_1 m'_1} b^{p_1\mu_1 *}_{l_1 h_1 m_1} b^{p\mu *}_{l'h'm'} b^{p\mu}_{lhm} a^{p_1\mu_1^*}_{l_1 h_1, l'_1 h'_1}(k) a^{p\mu}_{lh,l'h'}(k)\times \\ & (l_1 0 l 0 \mid L0)(l'_1 0 l' 0 \mid L0)(l_1 - m_1 l m \mid L - M)(l'_1 m'_1 l' m' \mid LM) \end{aligned} \tag{17}$$

where $(j_1 m_1 j_2 m_2 \mid j_3 m_3)$ are the usual Clebsch-Gordan coefficients and the auxiliary amplitudes $a^{p\mu}_{lh,l'h'}(k)$ are defined as

$$a^{p\mu}_{lh,l'h'}(k) \;=\; -\frac{\sqrt{\pi^3}}{k} i^{l'-l}\sqrt{2l'+1} T^{p\mu\,(S_n)}_{k,lh;l'h'}. \tag{18}$$

III. Computational details

In our study U is an optical potential which includes both an exact static-exchange part and a parameter-free correlation-polarization (CP) contribution. Following the prescription of Padial and Norcross [20], the correlation-polarization effects are introduced in the potential through a parameter-free model which combines the target correlation calculated from the local electron-gas theory for short distances with the asymptotic form of the polarization potential, given (for T_d molecules) by:

$$v_p(\vec{r}) = -\frac{1}{2}\frac{\alpha_0}{r^4}, \tag{19}$$

where α_0 is the spherical part of the molecular dipole polarizability. In our calculations the experimental value $\alpha_0 = 17.5$ a.u. was taken [47]. An SCF wavefunction for methane ground state is obtained and is used to generate the static-exchange-polarization potential. In Table 1 we show the contracted Cartesian Gaussian basis set used in this calculation. At the equilibrium $C-H$ bond distance ($R_{C-H} = 2.0503$ a$_0$) this basis set gives an SCF energy of -40.1987 a.u. which can be compared with the -40.2155 a.u. value of Nishimura and Itikawa [39]. In the present calculation the cutoff parameter used in the expansions of the target bound orbitals and of the static plus CP potential is $l_c = 16$. All possible values of $h \leq l$ are retained. With this cutoff, the normalization of all bound orbitals is better than 0.999. In SVIM calculations, we have limited the partial-wave expansions to $l_c = 12$ for energies $E_0 \geq 30$ eV, and to $l_c = 7$ for lower energies. In Table 2 we show the basis set R$_o$ used for the trial scattering functions. All the SVIM calculations are converged within four iterations.

Table 1: Cartesian gaussian functions used in the SCF calculations.

Atom	s		p		d	
	Exp.	Coeff.	Exp.	Coeff.	Exp.	Coeff.
C	4232.61	0.006228	18.1557	0.039196		
	634.882	0.047676	3.98640	0.244144		
	146.097	0.231439	1.14290	0.816775		
	42.4974	0.789108				
	14.1892	0.791751				
	1.96660	0.321870				
	5.14770	1.000000	0.35940	1.000000	1.500	1.000000
	0.49620	1.000000	0.11460	1.000000	0.750	1.000000
	0.15330	1.000000	0.04584	1.000000	0.300	1.000000
	0.06132	1.000000	0.02000	1.000000		
H	33.6444	1.000000	1.00000	1.000000		
	5.05796	1.000000	0.50000	1.000000		
	1.14680	1.000000	0.10000	1.000000		
	0.321144	1.000000				
	0.101309	1.000000				

Table 2: **Basis set used for the initial scattering functions.**

Scattering Symmetry	Center	Cartesian Gaussian Function[a]	Exponents
ka_1	C	s	2.0, 0.5, 0.1, 0.025
		z	2.0, 0.5, 0.05
		x^2,y^2,z^2	0.2, 0.05
	H	s	0.8, 0.2, 0.05
ka_2	C	xy	8.0, 2.0, 0.5, 0.12, 0.03
	H	x	4.0, 1.0, 0.25, 0.05, 0.01
	H	y	4.0, 1.0, 0.25, 0.05, 0.01
kb_1	C	y	8.0, 2.0, 0.5, 0.12, 0.03
	H	s	4.0, 1.0, 0.25, 0.05
	H	y	4.0, 1.0, 0.25, 0.05
kb_2	C	s	8.0, 2.0, 0.5, 0.1, 0.02
	C	x	4.0, 1.0, 0.25, 0.05
	H	s	2.0, 0.5, 0.1, 0.02
		x,z	4.0, 1.0,0.25, 0.05

[a]Cartesian Gaussian basis functions are defined as :
$\phi^{\alpha,\ell,m,n,\mathbf{A}}(\mathbf{r}) = N(x-\mathbf{A}_x)^\ell (y-\mathbf{A}_y)^m (z-\mathbf{A}_z)^n \exp(-\alpha|\mathbf{r}-\mathbf{A}|^2)$,
with N a normalization constant.

IV. Results and discussions

In Figs. 1 and 2 we present our calculated ICS and MTCS, respectively, for elastic e^-–CH_4 scattering, in the 1–50 eV energy range. The insets in both figures show the respective cross sections in the very low energy region. Some selected experimental data and the theoretical results of Jain [36] and of McNaugthen *et al.* [42] are also shown for comparison. In general, there is a good agreement among the various ICS data. Our calculation has predicted a shape resonance in ICS at around 10 eV which is in good agreement with the theoretical results of Jain [36], though shifted approximately 2 eV from the experimental value. In addition, our calculated Ramsauer minimum is located at around 0.4 eV, slightly lower than the experimental minimum at 0.6 eV. As it can be seen in Fig. 2, all the calculated MTCS agree quite well with each other within 15% and also with the experimental data of Boesten and Tanaka [32]. However, the measured data of Shyn and Cravens [31] are much lower, particularly in the region of the maximum, located at around 8 eV. Our theoretical results also show a minimum in the MTCS at around 0.3 eV which is in very good agreement with both calculated results.

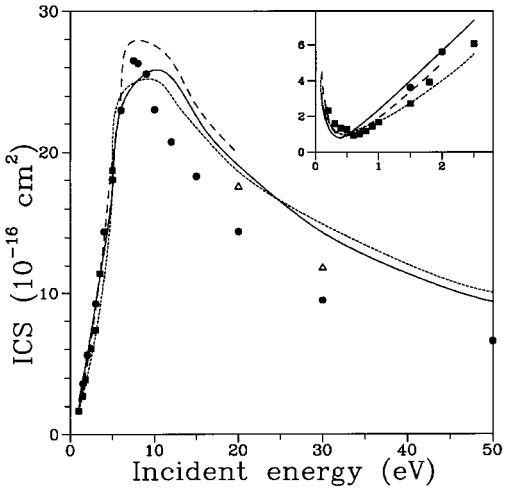

Figure 1: ICS for elastic e^-–CH_4 collision in the 0.1-50 eV energy range. Solid line, present results; dotted line, theoretical results of Jain (Ref. 36); short-dashed line, theoretical results of McNaughten *et al.* (Ref. 42); full circles, experimental data of Boesten and Tanaka (Ref. 32); full squares, experimental data of Sohn *et al.* (Ref. 30); open triangles, experimental data of Vuskovic and Trajmar (Ref. 29). Same symbols are used in the inset.

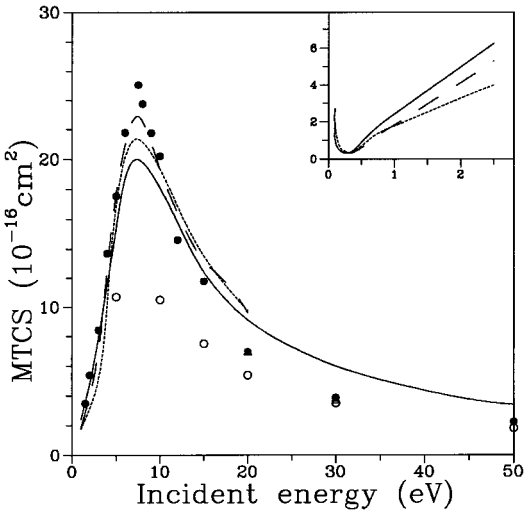

Figure 2: MTCS for elastic e^-–CH_4 collision. Symbols are the same as in figure 1, except: open circles, experimental data of Shyn and Cravens (Ref. 31).

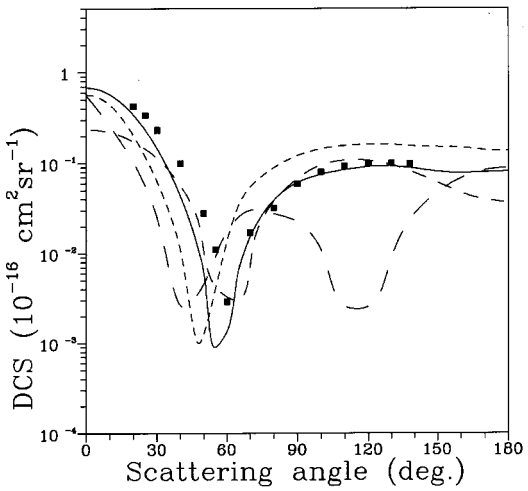

Figure 3: DCS for elastic e^-–CH_4 collision at 0.5 eV. Solid line, present results ; short-dashed line, theoretical results of Gianturco *et al.* (Ref. 43); dashed line, theoretical results of Lengsfield III *et al.* (Ref. 44); long-dashed line, theoretical results of Nestmann *et al.* (Ref. 45); full squares, experimental data of Sohn *et al.* (Ref. 30).

In Fig. 3 we show our calculated DCS for elastic e^-–CH_4 scattering at the electron impact energy of 0.5 eV, along with the experimental data of Sohn *et al.*

[30] as well as with some recent theoretical results [42-44]. The deep minimum at 60^o in the measured data is fairly well reproduced by the calculations. Nevertheless, the R-matrix calculation has also shown a second minimum at around 110^o, neither seen in the measured nor in all other theoretical data. Quantatively, our calculated results are also in general good agreement with the experimental data, particularly for scattering angles above 70^o.

In Fig. 4 our calculated DCS at 1.0 eV are compared with the experimental data of Sohn *et al.* [30] and the theoretical results from Jain [36], McNaughten *et al.* [42] and Lengsfield III *et al.* [44]. Our calculated SE results are also included in this figure. Again, the deep minimum at around 35^o in the experimental data is well reproduced by all calculations which include polarization effects. In particular, our static-exchange plus correlation-polarization calculation shows a very good agreement with the experimental results at the region of the minimum. As expected, the SE calculation was unable to reproduce this feature.

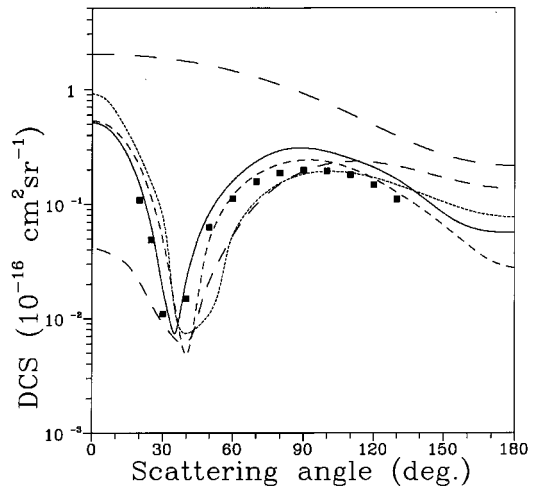

Figure 4: DCS for elastic e^-–CH_4 collision at 1.0 eV. Solid line, present results; dotted line, theoretical results of Jain (Ref. 36); short-dashed line, theoretical results of McNaughten *et al.* (Ref. 42) ; dashed line, theoretical results of Lengsfield III *et al.* (Ref. 44); long-dashed line, present results, static-exchange approximation; full squares, experimental data of Sohn *et al.* (Ref. 30).

Figures 5-8 show our calculated DCS for elastic e^-–CH_4 scattering at 5, 10, 20 and 50 eV, respectively, along with some available experimental [21, 28-32, 35] and theoretical [36, 39, 41-45] results. In general our calculated DCS agree very well with the measured data both qualitatively and quantitatively, except at 50 eV, where the quantitative agreement is only reasonable. The agreement with other theoretical results is also quite good.

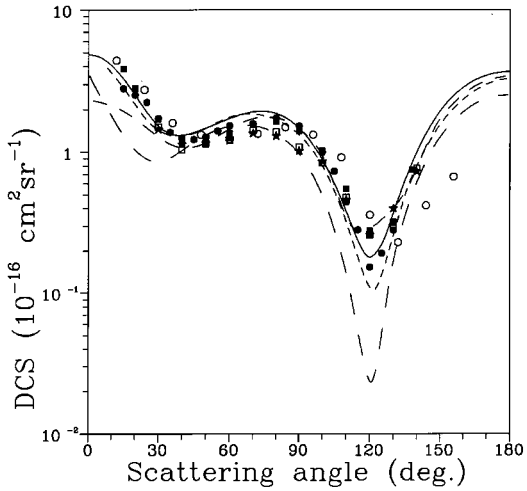

Figure 5: DCS for elastic e^-–CH_4 collision at 5.0 eV. Symbols are the same as in figure 3, except: full cirles, experimental data of Boesten and Tanaka (Ref. 32); open circles, experimental data of Shyn and Cravens (Ref. 31); open squares, experimental data of Tanaka *et al.* (Ref. 28); full stars, experimental data of Mapstone and Newell (Ref. 35).

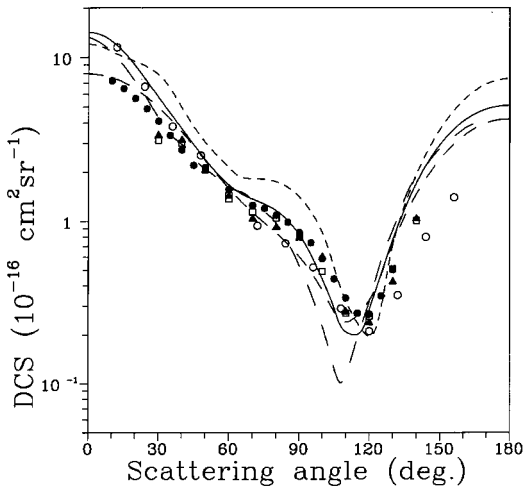

Figure 6: DCS for elastic e^-–CH_4 collision at 10.0 eV. Solid line, present results; short-dashed line, theoretical results of McNaughten *et al.* (Ref. 42); dashed line, theoretical results of Bettega *et al.* (Ref. 40); long-dashed line, theoretical results of Nishimura and Itikawa (Ref. 39). Symbols for experimental data are the same as in figure 5, except: full triangles, experimental data of Curry *et al.* (Ref. 21).

For the sake of completeness, in Table 3 we also present our calculated DCS, ICS, and MTCS for energies ranging from 0.1 to 50 eV.

In summary, the newly extended version of the SVIM codes which accounts for the correlation-polarization effects is applied by the first time to study the elastic electron scattering by a nonplanar molecule. More especifically, we have calculated ICS, MTCS and DCS for elastic e^-–CH_4 scattering, over a wide range of incident electron energies. In general our calculated results are in very good agreement with experimental and theoretical data reported in the literature which demonstrates that our new computational codes are highly reliable. Applications of these codes to other molecular systems are underway.

Table 3: **DCS, ICS and MTCS (in 10^{-16} cm^2) for elastic e$^-$–CH$_4$ scattering**

Angle	E_0 (eV)								
(deg)	0.1	0.2	0.3	0.4	0.5	0.6	0.7	0.8	1.0
0	1.055	0.9504	0.853	0.727	0.683	0.639	0.599	0.565	0.516
10	1.009	0.8716	0.757	0.627	0.574	0.525	0.481	0.443	0.388
20	0.889	0.6811	0.540	0.406	0.342	0.288	0.242	0.204	0.151
30	0.734	0.4782	0.327	0.206	0.146	0.101	0.067	0.043	0.181
40	0.584	0.3203	0.181	0.087	0.044	0.018	0.005	0.003	0.022
50	0.458	0.2121	0.095	0.030	0.006	0.001	0.009	0.027	0.084
60	0.360	0.1366	0.044	0.005	0.001	0.015	0.040	0.074	0.160
70	0.283	0.0821	0.014	0.001	0.015	0.045	0.085	0.131	0.236
80	0.223	0.0448	0.002	0.009	0.039	0.081	0.129	0.182	0.293
90	0.176	0.0223	0.001	0.022	0.061	0.107	0.157	0.208	0.310
100	0.139	0.0099	0.005	0.034	0.075	0.120	0.165	0.208	0.288
110	0.110	0.0035	0.011	0.043	0.084	0.125	0.162	0.195	0.250
120	0.088	0.0007	0.019	0.051	0.091	0.126	0.155	0.178	0.209
130	0.071	0.0003	0.025	0.056	0.092	0.121	0.141	0.154	0.165
140	0.060	0.0011	0.029	0.056	0.087	0.109	0.120	0.125	0.120
150	0.051	0.0020	0.032	0.054	0.081	0.096	0.101	0.099	0.084
160	0.046	0.0031	0.034	0.054	0.078	0.089	0.090	0.084	0.064
170	0.043	0.0041	0.037	0.057	0.079	0.089	0.088	0.080	0.057
180	0.042	0.0045	0.039	0.058	0.081	0.090	0.088	0.080	0.056
ICS	3.31	1.41	0.92	0.80	0.97	1.21	1.48	1.76	2.36
MTCS	1.79	0.38	0.32	0.52	0.89	1.25	1.58	1.88	2.41

Table 3: **cont'd**

Angle	E_0 (eV)								
(deg)	2.5	3.5	5.0	7.5	10.0	15.4	20.0	30.0	50.0
0	0.862	2.357	4.861	10.90	14.23	16.37	16.98	20.01	20.43
10	0.633	1.647	4.067	9.50	12.52	14.21	14.45	14.74	13.55
20	0.266	0.759	2.529	6.58	8.90	9.75	9.36	7.55	5.21
30	0.202	0.520	1.532	4.15	5.74	6.02	5.37	3.84	2.06
40	0.423	0.663	1.321	2.78	3.69	3.67	3.09	1.92	0.90
50	0.699	1.029	1.482	2.11	2.39	2.15	1.73	1.07	0.57
60	0.924	1.362	1.732	2.11	1.67	1.25	0.97	0.66	0.39
70	1.076	1.544	1.927	1.85	1.37	0.85	0.65	0.46	0.26
80	1.097	1.514	1.878	1.66	1.16	0.65	0.51	0.36	0.17
90	0.949	1.237	1.478	1.23	0.82	0.47	0.38	0.27	0.11
100	0.691	0.849	0.884	0.65	0.44	0.33	0.31	0.24	0.11
110	0.430	0.467	0.384	0.23	0.21	0.31	0.33	0.25	0.14
120	0.233	0.211	0.180	0.20	0.28	0.40	0.40	0.33	0.20
130	0.124	0.179	0.374	0.70	0.77	0.65	0.53	0.41	0.25
140	0.120	0.370	0.999	1.77	1.72	1.10	0.78	0.50	0.29
150	0.210	0.728	1.927	3.21	2.95	1.64	1.06	0.59	0.36
160	0.332	1.111	2.845	4.60	4.09	2.09	1.25	0.62	0.37
170	0.418	1.423	3.462	5.53	4.85	2.34	1.31	0.67	0.41
180	0.446	1.558	3.670	5.84	5.10	2.41	1.32	0.72	0.47
ICS	7.37	11.25	17.48	24.80	25.83	22.14	19.05	14.33	9.36
MTCS	6.24	9.75	15.40	19.98	18.08	12.07	9.12	6.00	3.40

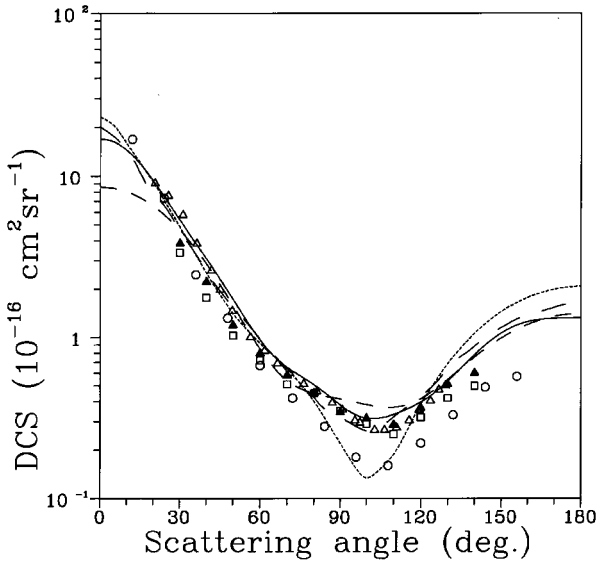

Figure 7: DCS for elastic e^-–CH_4 collision at 20.0 eV. Symbols are the same as in figure 6, except: dotted line, theoretical results of Jain (Ref. 36); open triangles, experimental data of Vuskovic and Trajmar (Ref. 29).

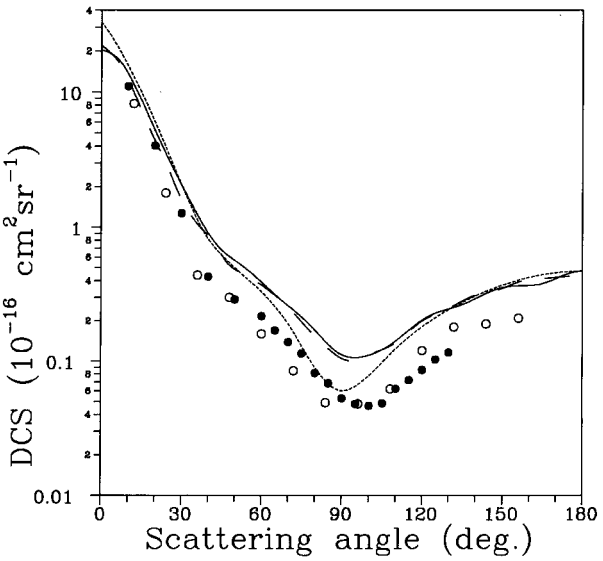

Figure 8. DCS for elastic e^-–CH_4 collision at 50.0 eV. Solid line, present results; dotted line, theoretical results of Jain (Ref. 36); long-dashed line, theoretical results of Nishimura and Itikawa (Ref. 39); full cirles, experimental data of Boesten and Tanaka (Ref. 32); open circles, experimental data of Shyn and Cravens (Ref. 31).

Acknowlegments

The present work was partially supported by the Brazilian agencies FAPESP, CNPq, and FINEP-PADCT.

References

[1] R.R. Lucchese, G. Raseev, and V. McKoy, Phys. Rev. A **25** 2572 (1982).

[2] R.R. Lucchese and V. McKoy, Phys. Rev. A **25** 1963 (1982).

[3] M.-T. Lee, L.M. Brescansin, M.A.P. Lima, L.E. Machado and E.P. Leal, J. Phys. B: At. Mol. Phys. **23** 4331 (1990).

[4] L.M. Brescansin, M.A.P. Lima, L.E. Machado and M.-T. Lee, Braz. J. Phys. **22** 221 (1992).

[5] L.E. Machado, M.-T. Lee, L.M. Brescansin, M.A.P. Lima and V. McKoy, Phys. B: At. Mol. Opt. Phys. **28** 467 (1995).

[6] L.E. Machado, E.P. Leal, M.-T. Lee and L.M. Brescansin, J. Mol. Struct. (THEOCHEM) **335** 37 (1995).

[7] R.R. Lucchese and V. McKoy, Phys. Rev. A **26** 1992 (1982).

[8] R.R. Lucchese and V. McKoy, Phys. Rev. A **28** 1382 (1993).

[9] M.E. Smith, V. McKoy, and R.R. Lucchese, J. Chem. Phys. **82** 195 (1985).

[10] M. Braunstein, V. McKoy, L.E. Machado, L.M. Brescansin, and M.A.P. Lima, J. Chem. Phys. **89** 2998 (1988).

[11] L.E. Machado, L.M. Brescansin, M.A.P. Lima, M. Braunstein and V. McKoy, J. Chem. Phys. **92** 2362 (1990).

[12] M.-T. Lee and V. McKoy, Phys. Rev. A **28** 697 (1983).

[13] M.-T. Lee, L.M. Brescansin, and M.A.P. Lima, J. Phys. B: At. Mol. Phys. **23** 3859 (1990).

[14] M.-T. Lee, L.M. Brescansin, M.A.P. Lima, L.E. Machado, E.P. Leal, and F.B.C. Machado, J. Phys. B: At. Mol. Phys. **23** L233 (1990).

[15] M.-T. Lee, L.E. Machado, L.M. Brescansin, and G.D. Meneses, J. Phys. B: At. Mol. Phys. **24** 509 (1991).

[16] M.-T. Lee, S.E. Michelin, T. Kroin, L.E. Machado, and L.M. Brescansin, J. Phys. B: At. Mol. Opt. Phys. **28** 1859 (1995).

[17] M.-T. Lee, A.M. Machado, M. Fujimoto, L.E. Machado, and L.M. Brescansin, J. Phys. B: At. Mol. Phys. **29** 4285 (1996).

[18] S.E. Michelin, T. Kroin, M.-T. Lee, and L.E. Machado, J. Phys. B: At. Mol. Phys. **30** 2001 (1997).

[19] R.R. Lucchese, D.K. Watson, and V. McKoy, Phys. Rev. A **22** 421 (1980).

[20] N.T. Padial and D.W. Norcross, Phys. Rev. A **29** 1742 (1984).

[21] P.J. Curry, S. Newell, and A.C. Smith, J. Phys. B: At. Mol. Phys. **18** 2303 (1985).

[22] W.L. Morgan, Plasma Chem. Plasma Process **12** 477 (1992).

[23] H. Tawara, Y. Itikawa, H. Nishimura, H. Tanaka, and Y. Nakamura, Atomic and Plasma-Material Interaction Data for Fusion (Nucl. Fusion Suppl.)] 2 41 (1992).

[24] R.B. Brode, Phys. Rev. **25** 636 (1925).

[25] E. Bruche, Ann. Phys. Lpz. **83** 1065 (1927).

[26] E. Bruche, Ann. Phys. Lpz. **4** 387 (1930).

[27] C. Ramsauer and R. Kollath, Ann. Phys. Lpz. **4** 91 (1930).

[28] H. Tanaka, T. Okada, L. Boesten, T. Suzuki, T. Yamamoto, and M. Kubo, J. Phys. B: At. Mol. Phys. **15** 3305 (1982).

[29] L. Vuskovic and S. Trajmar, J. Chem. Phys. **78** 4947 (1983).

[30] W. Sohn, K.-H. Kochem, K.-M. Scheuerlein, K. Jung, and H. Ehrhardt, J. Phys. B: At. Mol. Phys. **19** 3625 (1986).

[31] T.W. Shyn and T.E. Cravens, J. Phys. B: At. Mol. Opt. Phys. **23** 293 (1990).

[32] L. Boesten and H. Tanaka, J. Phys. B: At. Mol. Phys. **24** 821 (1991).

[33] I. Kanik, S. Trajmar, and J.C. Nickel, J. Geophys. Res. **98** 7447 (1993).

[34] S.L. Lunt, J. Randell, J.P. Ziesel, G. Mrotzek, and D. Field, J. Phys. B: At. Mol. Opt. Phys. **27** 1407 (1994).

[35] B. Mapstone and W.R. Newell, J. Phys. B: At. Mol. Opt. Phys. **25** 491 (1992).

[36] A. Jain, Phys. Rev. A **34** 3707 (1986).

[37] F.A. Gianturco and S. Scialla, J. Phys. B: At. Mol. Phys. **20** 3171 (1987).

[38] F.A. Gianturco, A. Jain, and L.C. Pantano, J. Phys. B: At. Mol. Phys. **20** 571 (1987).

[39] T. Nishimura and Y. Itikawa, J. Phys. B: At. Mol. Opt. Phys. **27** 2309 (1994).

[40] M.H.F. Bettega, A.P.P. Natalense, M.A.P. Lima and L.G. Ferreira, J. Chem. Phys. **103** 10566 (1995).

[41] M.A.P. Lima, T.L. Gibson, W.M. Huo, and V. McKoy, Phys. Rev. A **32** 2696 (1985).

[42] P. McNaughten, D.G. Thompson, and A. Jain, J. Phys. B: At. Mol. Opt. Phys. **23** 2405 (1990).

[43] F.A. Gianturco, J.A. Rodrigues-Ruiz, and N. Sanna, J. Phys. B: At. Mol. Opt. Phys. **28** 1287 (1995).

[44] B.H. Lengsfield III, T.N. Rescigno, and W.C. McCurdy, Phys] Rev. A **44** 4296 (1991).

[45] B.N. Nestmann, K. Pfingst, and S.D. Peyerimhoff, J. Phys. B: At. Mol. Opt. Phys. **27** 2297 (1994).

[46] P.G. Burke, N. Chandra, and F.A. Gianturco, J. Phys. B: At. Mol. Phys. **5** 2212 (1972).

[47] Landolt Börnstein: *Zahlenwerte und Funktionen* vol 1 part 3 (Berlin: Springer Verlag) p 511 (1951).